BEAM-INDUCED HEATING ANALYSIS AND OPTIMIZATION OF THE STRIPLINE KICKER FOR THE STCF*

B. Zhu, Y. Liu, X. Li, Y. Wang, J. Yang†, K. Fan‡, State Key Laboratory of Advanced Electromagnetic Technology (Huazhong University of Science and Technology), Wuhan, China

Abstract

The Super Tau-Charm Facility (STCF) is a high-luminosity electron–positron collider currently under design, featuring a single-bunch charge of up to 8 nC and an average beam current as high as 2 A. The swap-out injection scheme imposes stringent requirements on the stripline kicker (SLK), particularly regarding beam-induced heating effects under high-current operation. In this work, the design and optimization of the STCF SLK are presented, with special emphasis on impedance reduction and thermal-effect mitigation. Based on theoretical analysis and CST simulations, the loss factor, total parasitic power loss, and electrode power dissipation are systematically evaluated. The optimized structure with tapered transitions reduces the loss factor and electrode thermal power deposition significantly. Further thermal and mechanical analyses show that the maximum electrode temperature and thermal deformation remain within acceptable limits, while their influence on the electromagnetic field distribution is negligible. The results demonstrate that the optimized SLK satisfies the operational requirements of the STCF under high beam current conditions.

INTRODUCTION

The Super Tau-Charm Facility (STCF) is a next-generation high-luminosity electron–positron collider with beam energies ranging from 1 to 3.5 GeV and a stored beam current of up to 2 A. Owing to the limited dynamic aperture of the storage ring, both off-axis and swap-out injection schemes are under consideration. In particular, swap-out injection requires the kicker system to achieve high injection efficiency while minimizing perturbation to the stored beam and preserving collider luminosity. This operating mode requires the stripline kicker (SLK) to handle a single-bunch charge of 8.34 nC with a bunch spacing of only 4 ns, imposing stringent requirements on the pulse response, electromagnetic stability, and thermal reliability of the kicker system.

At such high beam current, beam–structure interactions can generate substantial beam coupling impedance, resulting in significant parasitic power deposition on the kicker electrodes. The associated temperature rise and thermal deformation of the kicker electrodes may distort the electromagnetic field distribution, degrade kicker performance, and compromise long-term operational stability. Consequently, suppression of beam-induced heating and optimization of impedance characteristics are critical challenges in the SLK design for STCF.

This work presents the design and optimization of the STCF stripline kicker with focus on impedance reduction and thermal-effect suppression. Electromagnetic properties, beam-induced loss, thermal behavior, and thermomechanical deformation are analyzed using theory and CST simulations, and the impact of thermal deformation on electromagnetic performance is evaluated.

DESIGN OF STCF STRIPLINE KICKER

Structural Design

The swap-out injection scheme for the STCF collider ring is currently under preliminary design and optimization. The present configuration adopts five SLKs, each with an effective length of 0.3 m, to provide a total deflection of 2.5 mrad for 3.5 GeV electron and positron beams, corresponding to 0.5 mrad per SLK [1]. The principal design parameters of the STCF SLK are summarized in Table 1.

Table 1: Main Parameters of the STCF Stripline Kicker

Parameter	Value
Injection Energy E [GeV]	3.5
Total Deflection Angle [mrad]	2.5
Number of Kicker	5
Effective Length of per Kicker [m]	0.3
Peak Pulsed Voltage [kV]	17.5
Odd-mode Impedance [Ω]	50
Even-mode Impedance [Ω]	<65
Pulse Rise/Fall Time [ns]	≤2
Pulse Flat-top Time [ns]	≥2
Total Pulse Width [ns]	≤6

The SLK uses an elliptical vacuum chamber with "fender" structures to improve even-mode impedance matching [2]. D-shaped electrodes enhance field uniformity, and tapered transitions at both ends reduce beam-induced heating and impedance discontinuities. The cross-section and prototype are shown in Fig. 1.

*Work supported by National key research and development program of China 2022YFA1602202
† jyang@hust.edu.cn
‡ kjfan@hust.edu.cn

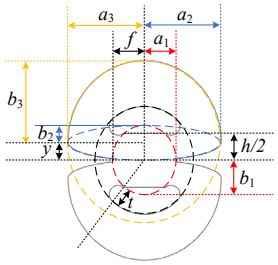

(a)

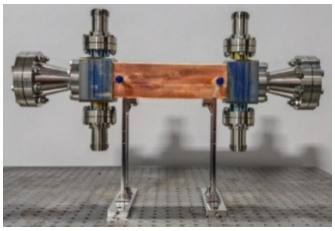

(b)

Figure 1: Structure of Stripline Kicker: (a) The cross-sectional structure; (b) Prototype.

Measurement Results

The simulated and measured characteristic impedances are shown in Fig. 2. The measured odd-mode and even-mode impedances are 50.37 Ω and 60.01 Ω, respectively, in good agreement with the design targets. The discrepancies between simulation and measurement are mainly attributed to machining tolerances, assembly accuracies, interface impedance mismatches, and parasitic effects introduced by the measurement cables. Nevertheless, the overall agreement confirms the validity of the electromagnetic design and simulation model.

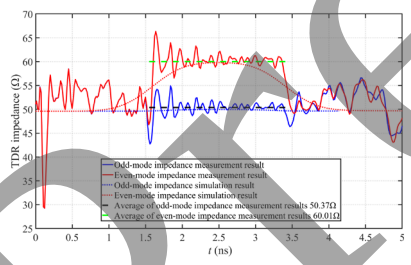

Figure 2: The simulated and measured results of characteristic impedances.

The measured pulse waveforms before and after transmission through the SLK are shown in Fig. 3. The measured rise time (10% – 90%) is 0.6 ns, the flat-top duration (90% – 90%) is 4.2 ns, the fall time (90% – 10%) is 1.2 ns, and the total pulse width (10% – 10%) is 6 ns. The output pulse amplitude exceeds 17.5 kV, demonstrating that the SLK satisfies the pulse-performance requirements for swap-out injection operation.

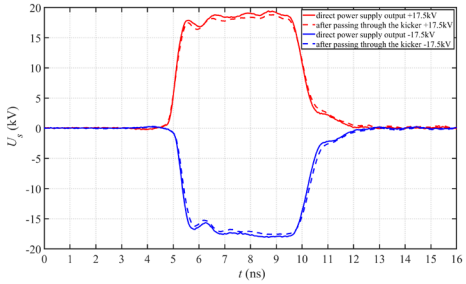

Figure 3: The measured pulse waveforms before and after transmission through the SLK.

BEAM-INDUCED HEATING ANALYSIS

To evaluate the thermal performance of the stripline kicker under high-current operation, the total parasitic power loss and the thermal power dissipated on the electrodes are calculated and compared for structures with and without tapered transitions. The resulting temperature rise and thermally induced deformation of the electrodes were subsequently investigated.

Power Dissipation Analysis

As the beam traverses the SLK, part of its energy is transferred to longitudinal wakefield, leading to parasitic power loss. The parasitic power loss P_{loss} is given by[3]:

$$P_{\mathrm{loss}} = \frac{k_{\mathrm{loss}} I^2 T_0}{\mathrm{M}} \tag{1}$$

where k_{loss} is the loss factor depending on the bunch length, T_0 is the revolution period, I is the beam current, and M is the number of bunches in the collider.

Table 2 summarizes the parasitic power loss for different injection energies based on beam parameters and the optimized loss factor k_{loss}. The maximum loss occurs at 2 GeV, which is therefore used for the subsequent thermal analysis.

Table 2: Beam Parameters and Parasitic Power Loss of the STCF Collider Ring at Different Energies

Parameter	Value			
E [GeV]	1	1.5	2	3.5
I [A]	1.1	1.7	2	2
σ_s [mm]	6.62	7.89	7.21	8.26
k_{loss} [V/pC]	0.2689	0.1894	0.2258	0.1731
T_0 [μs]	2.87	2.87	2.87	2.87
M	688	688	688	688
P_{loss} [W]	1357.28	2283.34	3767.71	2888.35

For the 2 GeV operating point, the beam current is $I = 2$ A and the bunch length is $\sigma_s = 7.21$ mm. With the introduction of tapered transitions, the loss factor decreases from 0.3385 V/pC to 0.2258 V/pC, corresponding to a reduction of 33.29%. According to Eq. (1), the corresponding parasitic power loss Ploss is consequently reduced from 5648.23 W to 3767.71 W, demonstrating the effectiveness of the tapered design in suppressing beam-induced power deposition.

To quantify the temperature rise of the SLK, the power dissipated on the electrodes was evaluated using CST simulations. The relationship between the bunch charge N_c and the beam current I is given by

$$I = \frac{MN_C}{T_0} \quad (2)$$

where M is the number of bunches and T_0 is the revolution period.

Substituting $I = 2$ A into Eq. (2) yields a bunch charge of N_c = 8.34 nC. Accordingly, a Gaussian bunch with N_c = 8.34 nC and σ_s = 7.21 mm is launched through the SLK in CST simulations. Figure 4 shows the power dissipated on the electrodes. The power density is concentrated primarily near the electrode gaps during bunch passage, after which the deposited power gradually decays with time.

The total power dissipated on the electrodes can be calculated as [4]:

$$P_{\text{stripline}} = M\left(\frac{N_e}{N_c}\right)^2 f_0 \int_0^t P_c(t)\mathrm{d}t \quad (3)$$

where N_e is the bunch charge (8.34 nC), N_c is the bunch charge set in the CST simulation, and P_c is the recorded power loss over a unit time interval.

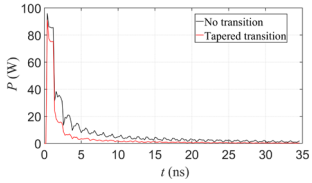

Figure 4: The power dissipated on the electrodes.

Substituting the operating parameters into the CST model, the electrode thermal power decreases from 62.57 W to 33.78 W after introducing tapered transitions, a 46.01% reduction. The remaining 3733.93 W is dissipated in the outer conductor and terminal loads [5].

Thermal and Mechanical Analysis

The steady-state temperature distribution of the optimized SLK was analyzed using the CST Thermal Solver. Water-cooling channels in the outer conductor maintain the vacuum chamber near 25 °C, so the PEC boundary in the model is set to 25 °C. Ceramic support plates (3 mm) provide both mechanical support and thermal conduction, and the copper electrodes are modeled as heat sources with a total power of 33.78 W (16.89 W per electrode). The maximum temperature reaches ~60 °C near the electrode center ($\Delta T \approx 35$ °C), as shown in Fig. 5. The resulting temperature field was imported into the CST Structural Mechanics Solver to evaluate thermal deformation, yielding a maximum displacement of 86.5 μm (Fig. 6).

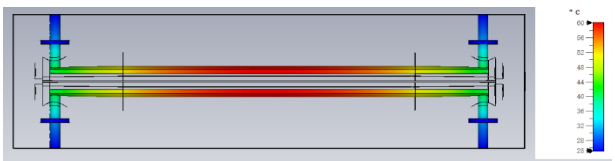

Figure 5: The steady-state temperature distribution.

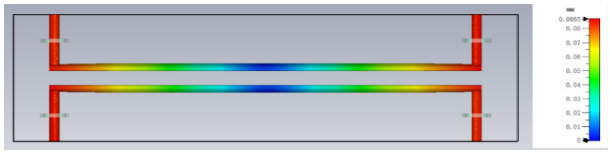

Figure 6: The resulting electrode deformation.

The deformed geometry was then analyzed in the CST Microwave Solver, and the transverse field distribution shows only negligible differences compared with the undeformed case (Fig. 7).

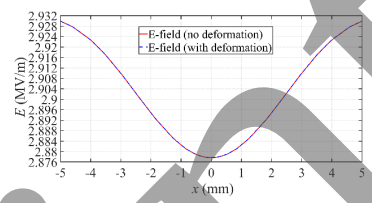

(a)

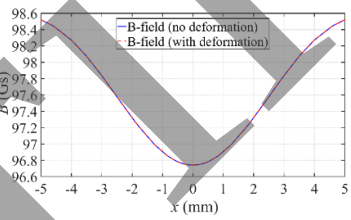

(b)

Figure 7: Comparison of results before and after electrode deformation: (a) Electric field; (b) Magnetic field.

Similarly, the electrode temperature rise $T_{max,}$ and deformation D_{max} of the SLK at different injection energies are obtained, as summarized in Table 3.

Table 3: Electrode Temperature and Deformation at Different Injection Energies

Parameter	Value			
E [GeV]	1	1.5	2	3.5
P_{loss} [W]	1357.28	2283.34	3767.71	2888.35
$P_{\text{stripline}}$ [W]	13.24	20.10	33.78	25.57
T_{max} [°C]	38.7	45.8	60.0	51.5
D_{max} [μm]	41.9	56.6	86.5	68.6

CONCLUSION

This work presents the design and optimization of the STCF stripline kicker under high beam-current conditions, with emphasis on beam-induced heating. Tapered transitions significantly reduce both loss factor and electrode power dissipation. Thermal–mechanical simulations show a maximum electrode temperature of ~60 °C and deformation of 86.5 μm under the worst case, with negligible impact on electromagnetic fields. The results confirm that the optimized SLK meets electromagnetic, thermal, and mechanical requirements for reliable STCF swap-out injection operation.

REFERENCES

[1] X.-C. Ai, Y. Zhang, H. Xu, *et al*., "Conceptual Design Report of Super Tau-Charm Facility: The Accelerator," *Nucl. Sci. Tech.*, vol. 36, 242, 2025 [Online]. doi:10.48550/arXiv.2509.11522

[2] C. B. Aguilar, "Development of stripline kickers for low emittance rings: Application to the beam extraction kicker for CLIC damping rings", Universitat de València, Valencia, Spain, 2015.

[3] W. Liu, "Design study of stripline nanosecond pulse kickers", University of Science and Technology of China, Hefei, China, 2020.

[4] N. Wang, S.K. Tian, L. Wang, *et al*., "Impedance optimization and measurements of the injection stripline kicker", *Phys. Rev. Accel. Beams*, vol. 24, no. 3, p. 034401, Mar. 2021. doi:10.1103/PhysRevAccelBeams.24.034401

[5] T. Gunzel, "Longitudinal impedance characterisation of the CLIC-stripline in view of its test in the ALBA storage ring", presented at Topical Workshop on Instabilities, Impedances and Collective Effects 2014 (TWIICE2014). Saint-Aubin, France, Jan. 2014.